Microscopic Theory of Josephson Mesoscopic Constrictions

A. Martín-Rodero, F. J. García-Vidal, and A. Levy Yeyati
Departamento de Física de la Materia Condensada C-XII, Facultad de Ciencias, Universidad Autónoma de Madrid, E-28049 Madrid, Spain
(Received 10 August 1993)

We present a microscopic theory for the dc Josephson effect in model mesoscopic constrictions. Our method is based on a nonequilibrium Green function formalism which allows for a self-consistent determination of the order parameter profile along the constriction. The various regimes defined by the different length scales (Fermi wavelength λ_F, coherence length ξ_0, and constriction length L_C) can be analyzed, including the case where all these lengths are comparable. For $\lambda_F \lesssim (L_C, \xi_0)$ phase oscillations with spatial period $\lambda_F/2$ can be observed. For $L_C > \xi_0$ solutions with a phase-slip center inside the constriction can be found, in agreement with previous phenomenological theories.

PACS numbers: 74.50.+r, 73.20.Dx, 85.25.Cp

The problem of dc Josephson transport through a superconducting constriction received considerable attention several years ago in the context of what was known as the theory of superconducting weak links [1]. In the last few years, there has been a renewed interest in the subject fostered by the advances in nanoscale technologies which would allow the fabrication of superconducting mesoscopic devices. Actually, some steps in this direction have already been taken with the development of a Josephson field effect transistor (JOFET) [2]. Another experimental situtation where this problem can be studied is that of a superconducting scanning tunneling microscope [3].

The relevant feature of such a mesoscopic device would be the phase coherence of both single electrons and Cooper pairs over a length comparable to the system size. This opens the possibility of observing novel interference phenomena when $\lambda_F \leq (\xi_0, \xi_N, L_C)$ (ξ_N denotes the normal electron coherence length). The case in which $L_C \ll \xi_0$ has been analyzed in a recent publication by Beenakker and van Houten [4]. In this regime the detailed form of the order parameter profile inside the constriction is irrelevant for the evaluation of the Josephson current. In the opposite limit ($L_C \gg \xi_0$) the superconducting phase would drop linearly along the constriction. A model for a superconducting point contact within this limit has been proposed by Furusaki *et al.* [5].

In the intermediate regime, in which all the relevant lengths can be comparable, one would need a self-consistent determination of the complex order parameter along the constriction. This poses a difficult task that has only been addressed within phenomenological Ginzburg-Landau theory [6] or with semiclassical treatments based on Boltzmann-type transport equations [7]. The aim of this work is to present a microscopic model for the self-consistent description of a Josephson constriction in all the relevant regimes.

We consider a model constriction like the one depicted in Fig. 1, which consists of a quasi-one-dimensional region of length L_C coupled to wider regions (L and R) which act as electron reservoirs. For simplicity, we assume a single quantum channel open for transport through the constriction (a generalization for the multichannel case is possible within the formalism outlined below). The reservoirs are homogeneous superconductors with a constant complex order parameter except near the interface region. Within our model, the constriction may be either superconducting or normal, although we will focus here on the superconducting case.

We use a local orbital representation for the description of the electronic states of the system. This representation is very well suited for the self-consistent determination of the order parameter profiles, provided that the pairing potential is assumed to be diagonal in this basis. This simplification does not affect in a relevant way the description of the superconducting state, which is controlled basically by a single parameter (the coherence length $\xi_0 \approx \hbar v_F/\pi\Delta$). In the lower part of Fig. 1 we represent, schematically, our discretized model constriction where the quasi-one-dimensional region is represented by a linear chain with N_C sites. For convenience, in the

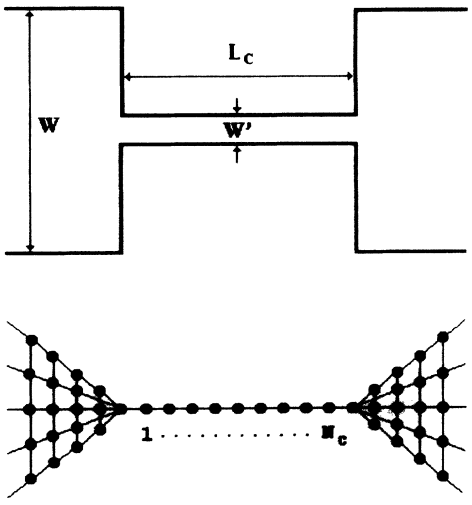

FIG. 1. Schematic representation of the model constriction considered in this paper.

0031-9007/94/72(4)/554(4)$06.00

numerical self-consistent calculations, the left and right reservoirs are represented by two Bethe lattices with coordination number $z+1$. The mean-field Hamiltonian for this model has the form

$$H = \sum_{i,\sigma}(\epsilon_i - \mu)c^\dagger_{i\sigma}c_{i\sigma} + \sum_{i\neq j,\sigma} t_{ij}c^\dagger_{i\sigma}c_{j\sigma} + \sum_i(\Delta^*_i c^\dagger_{i\downarrow}c^\dagger_{i\uparrow} + \Delta_i c_{i\uparrow}c_{i\downarrow}), \quad (1)$$

where the chemical potential μ is a constant throughout the whole system due to the absence of an applied voltage and will be taken as zero. The hopping parameters t_{ij} are only different from zero for nearest neighbors and the complex order parameters are given by

$$\Delta_i = -U_i\langle c^\dagger_{i\downarrow}c^\dagger_{i\uparrow}\rangle, \quad (2)$$

where U_i is the attractive e-e interaction at site i. The system defined by Eq. (2) provides the set of self-consistent conditions for obtaining the order parameter profile. We choose U_i and t_{ij} to be constant (U_L, U_C, U_R and t_L, t_C, t_R) inside each different region (left reservoir, constriction, right reservoir) in such a way as to fix the desired bulk values of Δ ($\Delta^0_L, \Delta^0_C, \Delta^0_R$) in the three separate regions. The hopping parameters, t_{ij}, can be chosen to be real and we take $t_L = t_R = t$ as the unit of energy. We denote by t_{LC} and t_{CR} the parameters coupling the left and right electrodes to the constriction.

In the absence of an applied bias voltage, the Josephson current through the constriction between sites i and $i+1$ is given by

$$I_i(t) = \frac{ie}{\hbar}t_C\sum_\sigma[\langle c^\dagger_{i\sigma}(t)c_{i+1\sigma}(t)\rangle - \langle c^\dagger_{i+1\sigma}(t)c_{i\sigma}(t)\rangle]. \quad (3)$$

One can show that I_i is independent of the chosen site, i.e., the continuity equation is fulfilled, only when the solution for the different Δ_i is fully self-consistent [8,9].

The averaged quantities appearing in Eqs. (2) and (3) are most conveniently expressed in terms of nonequilibrium Green functions $\mathbf{G}^{+-}$ [10], which in a Nambu (2×2) representation [11] are defined by

$$\mathbf{G}^{+-}_{i,j}(t,t') = i\begin{pmatrix} \langle c^\dagger_{j\uparrow}(t')c_{i\uparrow}(t)\rangle & \langle c_{j\downarrow}(t')c_{i\uparrow}(t)\rangle \\ \langle c^\dagger_{j\uparrow}(t')c^\dagger_{i\downarrow}(t)\rangle & \langle c_{j\downarrow}(t')c^\dagger_{i\downarrow}(t)\rangle \end{pmatrix}. \quad (4)$$

Then, the self-consistent Eq. (2) and the stationary current, Eq. (3), are given, in terms of the Fourier transform $\mathbf{G}^{+-}_{i,j}(\omega)$, by

$$\Delta_i = -\frac{U_i}{2\pi i}\int_{-\infty}^{\infty} d\omega[\mathbf{G}^{+-}_{ii}(\omega)]_{21}, \quad (5)$$

$$I_i = \frac{2e}{h}t_C\int_{-\infty}^{\infty} d\omega\left\{[\mathbf{G}^{+-}_{i+1,i}(\omega)]_{11} - [\mathbf{G}^{+-}_{i,i+1}(\omega)]_{11}\right\}. \quad (6)$$

All the different correlation functions appearing in Eqs. (5) and (6) can be obtained using conventional Green function techniques [12].

In the limit of $L_C \to 0$ it is possible to obtain analytical results for the Josephson current using this model. In this case, the self-consistent phase profile is well approximated by a step function between the L and R electrodes. Defining $\phi = \phi_L - \phi_R$ as the total phase diference, Eq. (6) can be written as

$$I = \frac{8e}{h}t^2_{LR}\sin(\phi)\int_{-\infty}^{\infty} d\omega \mathrm{Im}\left[\frac{\tilde{g}^r_{L,21}(\omega)\tilde{g}^r_{R,12}(\omega)}{D^r(\omega)}\right]f(\omega), \quad (7)$$

where t_{LR} is the coupling between the outermost sites on the left and right reservoirs, $f(\omega)$ is the Fermi distribution function; $\mathbf{g}^r_L$ and $\mathbf{g}^r_R$ are the retarded Green functions for the uncoupled electrodes (the tilde indicates that the phase factor has been removed, i.e., $g^r_{L,21} = e^{i\phi_L}\tilde{g}^r_{L,21}$ and $g^r_{R,12} = e^{-i\phi_R}\tilde{g}^r_{R,12}$), and

$$D^r(\omega) = \det[\mathbf{I} - t^2_{LR}\tau_3\mathbf{g}^r_L(\omega)\tau_3\mathbf{g}^r_R(\omega)], \quad (8)$$

τ_3 being the usual Pauli matrix.

It is interesting to analyze the transition from the tunnel to the contact regime as given by Eq. (7) (for simplicity we assume $\Delta^0_L = \Delta^0_R = \Delta$ and $\Delta \ll 1$). In the tunnel regime, $t_{LR} \ll 1$, $D^r \sim 1$, and one recovers the usual Josephson expression for a tunnel junction [13]

$$I(\phi) = \frac{\pi\Delta(T)}{2eR_N}\sin\phi\tanh\left[\frac{\Delta(T)}{2k_BT}\right], \quad (9)$$

where R_N is the normal resistance of the junction which is given by $R_N^{-1} = (2e^2/h)\alpha$, α being the normal transmission through the constriction which in our model adopts the simple form $\alpha = (4t^2_{LR}/zt^2)/(1+t^2_{LR}/zt^2)^2$ [14]. On the other hand, when approaching the contact limit, $\alpha \to 1$, the main contribution to the current comes from states inside the superconducting gap, which are given by the zeros of Eq. (8). These states are originated by multiple reflection processes at the interface region and give the following simple expression for the current

$$I(\phi) = \frac{\pi}{2eR_N}\frac{|\Delta(T)|^2}{|\epsilon(\phi)|}\sin(\phi)\tanh\left[\frac{|\epsilon(\phi)|}{2k_BT}\right], \quad (10)$$

$\epsilon(\phi) = \pm|\Delta(T)|\sqrt{1-\alpha\sin^2(\phi/2)}$ being the position of the states inside the gap . For the special case $\alpha = 1$, Eq. (10) yields $I(\phi) \sim \sin(\phi/2)$, which coincides with the result given in Refs. [4,15]. It is remarkable that, when $\alpha \to 0$, Eq. (10) tends exactly to Eq. (9), whose deduction involved no localized states. One can understand the equivalence between both ways of obtaining the tunnel limit by realizing that the localized states move towards the gap edges when $\alpha \to 0$, gradually becoming the band

edge singularities of the uncoupled system. These singularities gave the main contribution to the current when obtaining Eq. (9).

Let us turn our attention to the effects of self-consistency as one moves from the above regime to the opposite case, $L_C/\xi_0 \gg 1$. We have performed calculations for a wide range of constriction lengths and different values of the normal transmission parameter, α. The coordination number z on both electrodes has been taken equal to 3, which ensures a rapid convergence to the bulk values of the order parameter. The self-consistent order parameter profile is calculated in the following way: We first assume a given initial profile along the constriction. Then, we calculate the system Green functions for this profile which in turn yield the new order parameter profile using Eq. (5). This process is repeated until convergence is achieved.

In order to clarify the L_C/ξ_0 dependence of our results we have fixed $\Delta_C^0 = \Delta_L^0 = \Delta_R^0 = 0.05$ and $\lambda_F = 4a$ (a being the intersite distance) throughout the whole calculation. For the same reason we restrict ourselves to the zero temperature case in the present calculations. In Fig. 2 we show I versus ϕ curves chosen to represent typical behaviors found in the different physical regimes. Thus, Fig. 2(a) corresponds to the case of maximum transmission ($\alpha = 1$) , whereas Figs. 2(b) and 2(c) illustrate cases with decreasing α. In these figures we plot curves for different values of L_C/ξ_0, ranging from $L_C/\xi_0 = 0$ to $L_C/\xi_0 \gg 1$. We only represent the part of the curves with $I(\phi) \geq 0$.

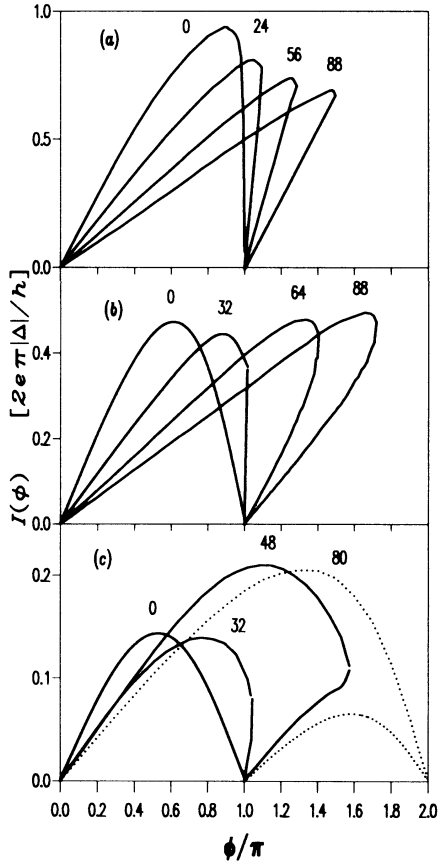

FIG. 2. Josephson current versus total phase difference for three different values of the transmission parameter α: (a) $\alpha = 1$, (b) $\alpha = 3/4$, and (c) $\alpha \simeq 1/12$. In cases (a) and (b) the hopping parameter between the constriction and the reservoirs (t_{LC} and t_{CR}) is equal to the intrachain hopping t_C [$t_C = \sqrt{z}$ for case (a) and $t_C = 1$ for case (b)], whereas in case (c) we take $t_C = 1$ and $t_{LC} = t_{CR} = 0.5$. The numbers above each curve indicate the number of sites within the constriction.

Several features are noticeable in these curves. First, when increasing L_C/ξ_0, a critical value $L_C/\xi_0 \sim 1$ is reached above which the function $I(\phi)$ becomes multivalued [1,6,9]. This situation corresponds to the appearance of a second kind, or "solitonic," solution with a phase slip center inside the constriction, in addition to the normal one consisting basically of a linear phase profile between the reservoirs. In Fig. 3 the two kinds of self-consistent profiles for $L_C > \xi_0$ are displayed. They correspond to $\phi \simeq \pi$ where the phase drop inside the constriction is specially sharp. It is worth noticing the appearance of oscillations of period $\lambda_F/2$ in both profiles (phase and modulus). This interference effect is a consequence of the phase coherence of the normal electrons along the constriction, analogous to the oscillations found in the electrochemical potential in normal mesoscopic wires [16,17]. On the other hand, the other relevant length scale, ξ_0, manifests itself in a clear way in the solitonic phase profile: one can

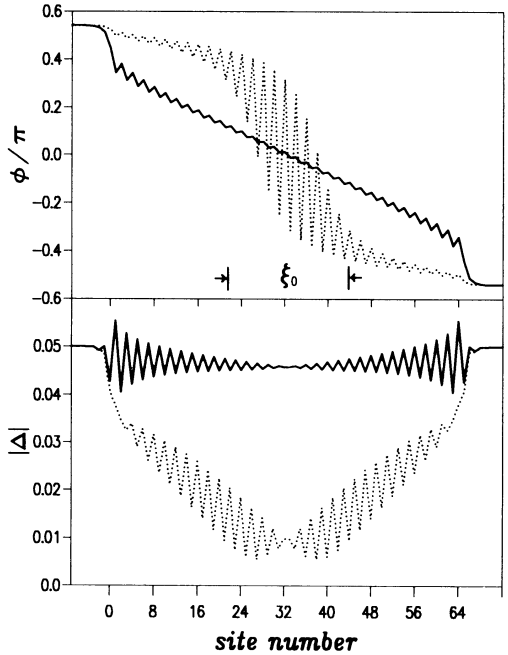

FIG. 3. Self-consistent order parameter phase and modulus profiles for the case $N_C = 64$ and $\phi = 3.4$ of Fig. 2(b). Solid and dotted lines correspond to the solution in the upper and lower branches of the $I(\phi)$ curve, respectively.

verify that the width of the phase-slip center is almost equal to ξ_0. The overall features of these solitonic solutions are in agreement with predictions made in previous phenomenological analysis [1,18].

It is interesting to observe the behavior of the maximum Josephson current, $I_{\max}$, as a function of L_C for the different situations represented in Fig. 2. In the case of maximum transmission [Fig. 2(a)] a slow decrease in $I_{\max}$ is observed for increasing L_C, with a limiting value corresponding to the critical current of the infinite one-dimensional chain. This monotonic decrease of $I_{\max}$ is not found when the transmission is lowered below a certain value. For instance, for the case of Fig. 2(b), $I_{\max}$ slightly increases with L_C, tending to the same limiting value as in Fig. 2(a).

Figure 2(c) corresponds to a somewhat different physical situation, in which a weaker coupling between the constriction and the reservoirs is considered. For sufficiently large L_C, this situation may be regarded as a case not far from two identical tunnel junctions connected in series, which would have a $I(\phi) \sim \sin(\phi/2)$ characteristic, whereas for $L_C < \xi_0$ the system behaves like a single junction with the usual $I(\phi) \sim \sin\phi$ form. The transition between these two regimes can be clearly observed in Fig. 2(c). Note that with increasing L_C, $I(\phi)$ becomes eventually multivalued, as in the previous cases. However, for large enough L_C [see case $N_C = 80$ in Fig. 2(c)], the solitonic branch does not merge in a continuous way into the "normal" one. Instead, both branches extend up to $\phi = 2\pi$ keeping a different character. In the lower branch, the region where the modulus of the order parameter nearly goes to zero tends to fill the whole constriction when $\phi \to 2\pi$.

In conclusion, we have presented a fully self-consistent description of the dc Josephson transport on a mesoscopic weak link. As a first check, the method has been applied to the case of a short constriction, recovering previously known results. On the other hand, we have analyzed the case where the constriction length is comparable or larger than the superconducting coherence length. To our knowledge, this is the first calculation of the self-consistent order parameter profiles and the current-phase relationship based on a microscopic model. The local character of our procedure makes it specially powerful for treating systems with a more complicated geometry in situations where the self-consistent variation of the order parameter plays a crucial role. For instance, using the present approach one would be able to address the problem of the proximity induced Josephson effect in a metal-superconductor nanojunction [19]. Work along this line as well as on the inclusion of a finite voltage for the study of the ac Josephson effect is under progress.

Support by Spanish CICYT (Contract No. PB89-0165) is acknowledged. The authors are indebted to F. Flores, F. Sols, J. Ferrer, and J. P. Hernández for stimulating discussions during the course of this work.

[1] For a review see K.K. Likharev, Rev. Mod. Phys. **51**, 101 (1979).

[2] C. Nguyen, J. Werking, H. Kroemer, and E.L. Hu, Appl. Phys. Lett. **57**, 87 (1990).

[3] C.J. Muller, J.M. Ruitenbeck, and L.J. de Jongh, Physica (Amsterdam) **191C**, 485 (1992); N. Agrait, J.G. Rodrigo, C. Sirvent, and S. Vieira, Phys. Rev. B **46**, 5814 (1992).

[4] C.W.J. Beenakker and H. van Houten, Phys. Rev. Lett. **66**, 3056 (1991); C.W.J. Beenakker, in *Proceedings of the 14th Taniguchi International Symposium on Physics of Mesoscopic Systems*, edited by H. Fukuyama and T. Ando (Springer, Berlin, 1992).

[5] A. Furusaki, H. Takayanagi, and M. Tsukada, Phys. Rev. Lett. **67**, 132 (1991).

[6] L.G. Aslamazov and A.I. Larkin, Pis'ma Zh. Eksp. Teor. Fiz. **9**, 150 (1969) [JETP Lett. **9**, 87 (1969)]; K.K. Likharev and L.A. Yacobson, Zh. Tekh. Fiz. **45**, 1503 (1975) [Sov. Phys. Tech. Phys. **20**, 950 (1975)].

[7] O. Kulik and A.N. Omel'yanchuk, Fiz. Nisk. Temp. **3**, 945 (1977); **4**, 296 (1978) [Sov. J. Low Temp. Phys. **3**, 459 (1977); **4**, 142 (1978)].

[8] G.E. Blonder, M. Tinkham, and T.M. Klapwijk, Phys. Rev. B **25**, 4515 (1982).

[9] J. Ferrer and F. Sols, Physica (Amsterdam) B (to be published).

[10] L.V. Keldysh, Zh. Eksp. Teor. Fiz. **47**, 1515 (1964) [Sov. Phys. JETP **20**, 1018 (1965)].

[11] Y. Nambu, Phys. Rev. **117**, 648 (1960).

[12] In the absence of an applied voltage the correlation functions $\mathbf{G}^{+-}(\omega)$ are given simply by $\mathbf{G}^{+-}(\omega) = f(\omega)[\mathbf{G}^a(\omega) - \mathbf{G}^r(\omega)]$. For a recursive method for obtaining $\mathbf{G}^{a,r}$ see, for instance, A. Levy Yeyati, Phys. Rev. B **45**, 14 189 (1992).

[13] V. Ambegaokar and A. Baratoff, Phys. Rev. Lett. **10**, 486 (1963); **11**, 104 (1963).

[14] J. Ferrer, A. Martín-Rodero, and F. Flores, Phys. Rev. B **38**, 10 113 (1988); A. Martín-Rodero, J. Ferrer, and F. Flores, J. Microsc. **152**, 316 (1988).

[15] G.B. Arnold, J. Low Temp. Phys. **59**, 143 (1985); J. Ferrer, Ph.D. thesis, Universidad Autónoma de Madrid, 1990 (unpublished).

[16] P. L. Pernas, A. Martín-Rodero, and F. Flores, Phys. Rev. B **41**, 8553 (1990).

[17] M. Buttiker, Phys. Rev. B, **40**, 3409 (1989); J.L. D'Amato and H. Pastawski, Phys. Rev. B **41**, 7411 (1990).

[18] L. Kramer and A. Baratoff, Phys. Rev. Lett. **38**, 518 (1977).

[19] A. Katalsky, A.W. Kleinasser, L.H. Greene, R. Bhat, F.P. Milliken, and J.P. Harbison, Phys. Rev. Lett. **67**, 3026 (1991); N. Agrait, J.G. Rodrigo, and S. Vieira, Phys. Rev. B **46**, 5814 (1992).